Bioconjugate Chemistry

Article

pubs.acs.org/bc

Enhancing Reactivity for Bioorthogonal Pretargeting by Unmasking Antibody-Conjugated *trans*-Cyclooctenes

Maha K. Rahim,[†] Rajesh Kota,[†] and Jered B. Haun*[,†,‡,§]

[†]Department of Biomedical Engineering, [‡]Department of Chemical Engineering and Materials Science, and [§]Chao Family Comprehensive Cancer Center, University of California, Irvine, Irvine, California 92697, United States

Supporting Information

ABSTRACT: The bioorthogonal cycloaddition reaction between tetrazine and *trans*-cyclooctene (TCO) is rapidly growing in use for molecular imaging and cell-based diagnostics. We have surprisingly uncovered that the majority of TCOs conjugated to monoclonal antibodies using standard amine-coupling procedures are nonreactive. We show that antibody-bound TCOs are not inactivated by *trans*−*cis* isomerization and that the bulky cycloaddition reaction is not sterically hindered. Instead, TCOs are likely masked by hydrophobic interactions with the antibody. We show that introducing TCO via hydrophilic poly(ethylene glycol) (PEG) linkers can fully preserve reactivity, resulting in >5-fold enhancement in functional density without affecting antibody binding. This is accomplished using a novel dual bioorthogonal approach in which heterobifunctional dibenzylcyclooctyne (DBCO)−PEG−TCO molecules are reacted with azido-antibodies. Improved imaging capabilities are demonstrated for different cancer biomarkers using tetrazine-modified fluorophore and quantum dot probes. We believe that the PEG linkers prevent TCOs from burying within the antibody during conjugation, which could be relevant to other bioorthogonal tags and biomolecules. We expect the improved TCO reactivity obtained using the reported methods will significantly advance bioorthogonal pretargeting applications.

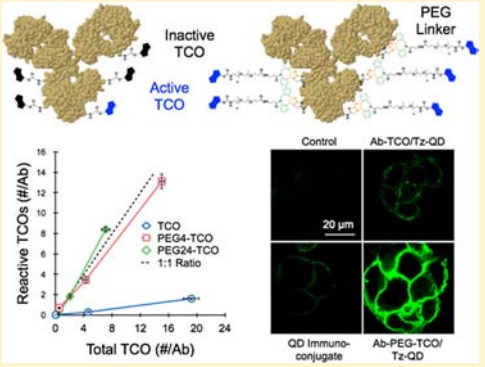

INTRODUCTION

There is currently strong interest in utilizing bioorthogonal chemistries to augment the detection of diseases both inside and outside of the body.[1−5] These works utilize the concept of pretargeting, where a chemically tagged affinity molecule such as a monoclonal antibody is first applied to mark the target site, followed by covalent attachment of the contrast agent.[6,7] Due to poor *in vivo* pharmacokinetics or other limitations of a traditional direct conjugate, pretargeting has been shown to improve imaging capabilities under different modalities in animal models.[8−16] Moreover, the small size of bioorthogonal reactants enable antibodies to act as scaffolds for the attachment of numerous nanomaterial probes to cells and microvesicles, leading to dramatic signal amplification for *in vitro* cultures and *ex vivo* human clinical specimens.[17−27]

Bioorthogonal pretargeting applications have predominantly employed the catalyst-free inverse-electron-demand Diels−Alder cycloaddition between 1,2,4,5-tetrazine and *trans*-cyclooctene (TCO) due to its high selectivity and unprecedented speed.[28,29] Specifically, the reaction between tetrazine/TCO is several orders of magnitude faster than tetrazine with other dienophiles such as norbornene and methyl-cyclopropene or alternative catalyst-free chemistries such as the strain-promoted azide/cyclooctyne reaction.[2,30−32] This rapid kinetics is critical to success in pretargeting scenarios, particularly within the body. The hydrophobic TCO is typically attached to monoclonal antibodies via standard amine-reaction to lysine residues, and TCO decorated antibodies have been shown to retain aqueous stability and binding affinity even at high modification levels.[9,10,15,17−27,29] However, there is a large discrepancy in the literature with respect to the number of TCO attachments that can be obtained, and results diverge depending on the method of analysis. Specifically, total TCO conjugations measured by mass spectrometry have been reported to be as high as 10−20,[17,18,20] whereas functional TCOs assessed by tetrazine reaction have been usually fewer than 6.[9,10,15,29] A potential explanation for these results is that a significant proportion of TCO attachments have been rendered nonreactive. Several mechanisms could be involved with TCO inactivation, including (1) conversion of TCO to the *cis* isoform that is orders of magnitude less reactive with tetrazine, (2) steric hindrance of the bulky cycloaddition reaction near the antibody surface, and (3) interaction of the hydrophobic TCO with external or even internal domains of the antibody. *Trans*−*cis* isomerizaton has been shown to occur on the order of hours in the presence of catalysts such as free thiols or transition metals bound to serum proteins *in vivo*,[31,33] although neither of these routes is expected for antibody conjugates directly after preparation. The tetrazine/TCO cycloaddition reaction results in a large, bulky dihydropyrazine product that

Received: December 20, 2014
Revised: January 10, 2015
Published: January 13, 2015

DOI: 10.1021/bc500605g
Bioconjugate Chem. 2015, 26, 352−360

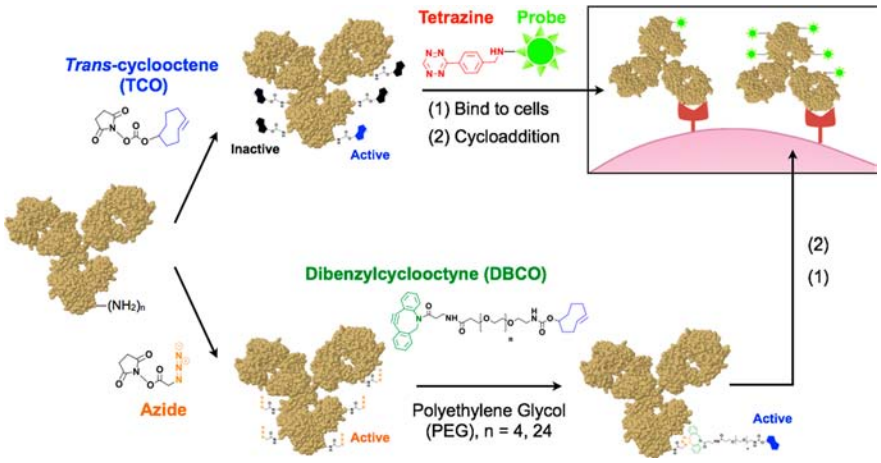

Figure 1. Direct conjugation of TCO to antibodies via standard amine-reaction results in both active (blue) and inactive (black) moieties. We report that hydrophilic PEG linkers can fully preserve TCO reactivity. TCO–PEGs were introduced by initially modifying the antibody with azides followed by reaction with heterobifunctional DBCO–PEG_n–TCO (n = 4 or 24). The improved reactivity obtained with the PEG linker will directly enhance binding of tetrazine-modified probes.

could be sterically hindered by the antibody surface. Steric effects have been noted to reduce the reaction rate of TCO with tetrazines containing bulky substituents, such as a *tert*-butyl group, and these effects were not observed for smaller cyclopropenes.[34] Finally, the hydrophobic TCO may simply bury within interior domains of the antibody to avoid the aqueous solvent. Further investigation into these potential inactivation mechanisms and overall TCO reactivity after attachment to monoclonal antibodies is needed to ensure that the remarkable speed and power of the tetrazine/TCO cycloaddition reaction translate to applications employing complex biomolecules. Placing the less hydrophobic tetrazine on the antibody could potentially alleviate some of these issues, but stability of TCO-modified secondary agents could be a major challenge, particularly for nanoparticles. We believe the focus should instead be on retaining TCO reactivity following bioconjugation, thereby maximizing the power of bioorthogonal pretargeting applications such as *in vivo* imaging and *ex vivo* nanoparticle amplification for cellular diagnostics.

A simple and straightforward strategy to increase TCO solubility and physically prevent interactions with the antibody is to append TCO via a hydrophilic polymer linker. Poly(ethylene glycol) (PEG) has a long history of use with antibodies for reducing immunogenicity and improving pharmacokinetics.[35] Furthermore, it is well-known that PEG can improve the solubility of hydrophobic molecules such as drugs, fluorophores, and biotin. For the hydrophobic fluorophore indocyanine green (ICG), short PEG linkers have been shown to reduce aggregation of antibody conjugates and prevent ICG quenching by aromatic amino acids.[36,37] Finally, it was recently demonstrated that attaching TCO via a PEG linker increased the rate of *trans–cis* isomerization in serum, presumably by making the TCO more accessible to protein-bound transition metals that can catalyze the conversion.[33] The PEG linker did not affect the reaction rate with tetrazine; however, the number of reactive TCOs attached to the antibody was not characterized. Thus, the activity of bioorthogonal reactants immediately after antibody conjugation has not been investigated to date. A potential drawback is that PEG linkers can block antibody binding, although this appears to be less of an issue for shorter PEGs less than 1000 Da.[38−40]

Herein, we characterize TCO reactivity on the surface of different monoclonal antibodies following standard amine-conjugation procedures. Surprisingly, we find that up to 90% of antibody-associated TCOs are nonfunctional. We present evidence that suggests TCOs are neither inactivated by *trans–cis* isomerization nor sterically hindered from cycloaddition reaction near the antibody surface; thus, we believe that inactive TCOs are masked by interactions with the antibody. Most importantly, we successfully restore reactivity by appending TCO using both short and long hydrophilic PEG linkers. We attach the PEG–TCO linkers via bioorthogonal reaction between azide and dibenzylcyclooctyne (DBCO), which is mutually orthogonal to the tetrazine/TCO chemistry.[41] This novel dual bioorthogonal approach involves first decorating the antibody with varying amounts of azide followed by cycloaddition reaction with heterobifunctional DBCO–PEG–TCO molecules (Figure 1). Overall improvements in functional TCO density are more than 10-fold in total and 5-fold without significant loss of antibody binding activity. Enhanced detection signals are also demonstrated for tetrazine-modified fluorophores and quantum dots (QD) using flow cytometry and confocal imaging. This work should significantly expand the power of bioorthogonal pretargeting applications such as *in vivo* molecular imaging and cell-based diagnostics utilizing chemical amplification of nanoparticle binding.

RESULTS AND DISCUSSION

We first set out to explore TCO reactivity using a mouse monoclonal antibody that is specific for the cancer biomarker EGFR. Total TCO modification levels were measured using matrix-assisted laser desorption/ionization time-of-flight (MALDI-TOF) mass spectrometry (Figure S2), whereas TCO reactivity was determined based on absorbance readings after complete reaction with tetrazine–Oregon Green 488. We found that TCO conjugation was efficient (Figure 2A), but, remarkably, only 10% of the moieties were functional (Figure 2B). Reactivity was identical when measured immediately following conjugation and after waiting up to 24 h (Figure 2C). This suggests that TCO was not inactivated by *trans–cis* isomerization, as this conversion has been shown to require significant amounts of time even in the presence of a catalyst. For example, 6 h or more is needed for full isomerization in the

DOI: 10.1021/bc500605g
Bioconjugate Chem. 2015, 26, 352−360

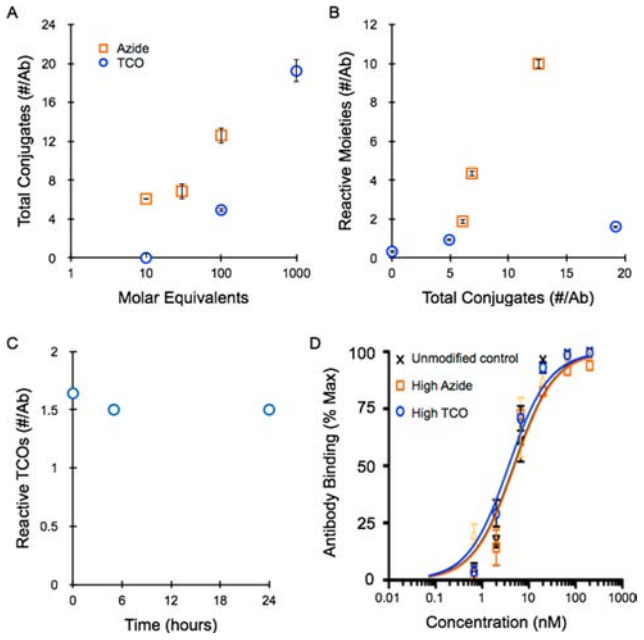

Figure 2. Conjugation of TCO and azide to an anti-EGFR antibody using standard amine-reaction procedures. (A) Total attachment levels determined by MALDI-TOF versus the number of reaction equivalents, showing that modification efficiencies are similar. (B) Reaction of the TCO−antibodies with tetrazine−fluorophore revealed that only 10% of the TCOs were functional. In contrast, nearly all azide modifications were reactive to DIBO−fluorophore. (C) Functional TCO level was similar on the anti-EGFR antibody immediately after treatment with NHS−TCO or after being maintained 5 and 24 h at room temperature, suggesting that TCOs were not inactivated by *trans*−*cis* isomerization. (D) Antibody binding affinity was not affected after modification with high levels of azide or TCO (K_D ~ 5 nM). Error bars represent the standard error of at least three independent experiments.

presence of free thiols at high concentrations and elevated temperatures or transition metals in serum.[31,33] To explore steric hindrance, we employed the strain-promoted bioorthogonal reaction between azide and cyclooctyne that also yields a bulky cycloaddition product. Azide conjugation efficiency was similar to the TCO (Figure 2A), but nearly all moieties could be reacted with dibenzocyclooctyne (DIBO)−Alexa Fluor 488 (Figures 2B). Discrepancies at low loadings were likely due to the small size of azide groups, which makes mass changes difficult to distinguish by MALDI-TOF. We expect that this result should extend to tetrazine/TCO cycloaddition, although the smaller azide could be less sensitive to sterics, as noted for methyl-cyclopropene in relation to TCO.[34] Interestingly, neither TCOs nor azides interfered with antibody binding affinity even at high modification levels (Figure 2D). This was determined using an indirect competitive binding assay with A431 epidermoid cancer cells. Fitting the binding data indicated equilibrium dissociation constants (K_D) were all close to 5 nM. On the basis of the above evidence, we speculated that hydrophobic TCOs were interacting with external or even internal domains of the antibody, masking it from tetrazine reaction. Internal burying could explain how an antibody decorated with almost 20 hydrophobic TCOs can remain stable in aqueous solution. To explore whether the presence of a polar solvent during conjugation procedures influenced TCO masking, we decreased the concentration of dimethylformamide (DMF) to <1%, but this had no effect on total modification levels and only slightly decreased reactive sites (Figure S3). Increasing DMF concentration or adding dimethyl sulfoxide (DMSO) during the reaction with tetrazine−Oregon Green 488 did reveal 30% more reactive TCOs (Figure S3). However, the majority remained inactive, and further increases in solvent destabilized the antibody. Further access to the masked TCOs could potentially be obtained using a more hydrophobic tetrazine conjugate such as a bodipy fluorophore.

We next explored whether introduction of TCO using hydrophilic PEG linkers could maintain reactivity. We chose to incorporate PEG−TCO onto the antibody using the mutually orthogonal azide/DBCO reaction to improve control over coupling density, as we have already established that azide is an ideal reactant on the antibody at varying densities (Figure 2B). We created heterobifunctional DBCO−PEG−TCO molecules with 4 and 24 polymer subunits by sequentially reacting amine−PEG−carboxylic acid with the same amine-reactive TCO employed for direct antibody conjugations. The carboxylic acid was then modified with amine-DBCO via *N*-hydroxysuccinimide (NHS) ester activated chemistry, and the resulting DBCO−PEG−TCO was reacted with azido-antibodies (Figure 1). Total loadings of the PEG_4 and PEG_{24} linkers were assessed by MALDI-TOF (Figures 3A and S2) and varied in a dose-dependent manner with the initial azide density. Attachment levels for the PEG_4−TCO were higher in all cases, with a maximum valency of 15 that was close to the 13 azides that were directly measured by MALDI-TOF. Conjugation of the PEG_{24}−TCO was less efficient, with values approximately one-half that of the PEG_4−TCO. It is unclear whether lower conjugation levels for the PEG_{24} were due to physical crowding or the presence of unreacted DBCO-amine in the preparation. Increasing linker concentration in the reaction did not affect results, however.

We next determined whether the PEG−TCO linkers interfered with antibody binding again using the indirect competitive assay with A431 cells. We found that binding at 10 μg/mL concentration was unaffected for both the PEG linkers until attachment levels exceeded 8 (Figure 3B). Further analysis of full binding profiles confirmed that affinity was close to control for 8 PEG_{24}−TCOs (K_D = 6 nM), but it was dramatically reduced for 15 PEG_4−TCOs (Figure 3C). Reduced binding in the latter case can be attributed either to decreased affinity or a population of permanently inactivated antibody, but, in either case, binding was almost fully recovered by increasing the antibody concentration to 30 μg/mL (Figure S4). Importantly, TCO moieties introduced via both PEG linkers were fully functional (Figure 3D). This was determined under pretargeting conditions, in which A431 cells were labeled with TCO−PEG−antibodies, reacted with tetrazine−Oregon Green 488 at 50 μM for 30 min in the presence of BSA, and analyzed by flow cytometry. The TCO−antibodies prepared by direct amine reaction were also evaluated and used to convert raw fluorescence signals (Figure S4) into the number of functional TCOs per antibody, after adjusting for antibody binding levels. These results were highly specific, as background signals from a nonbinding control antibody conjugated with TCO and PEG_{24}−TCO were similar to autofluorescence (Figure S4). In total, antibody reactivity enhancements were more than 10- and 5-fold for the 4 and 24 subunit PEGs, respectively. To illustrate these improvements, we performed confocal imaging of A431 cells labeled with TCO- or TCO−PEG-modified antibodies, followed by reaction with an

DOI: 10.1021/bc500605g
Bioconjugate Chem. 2015, 26, 352−360

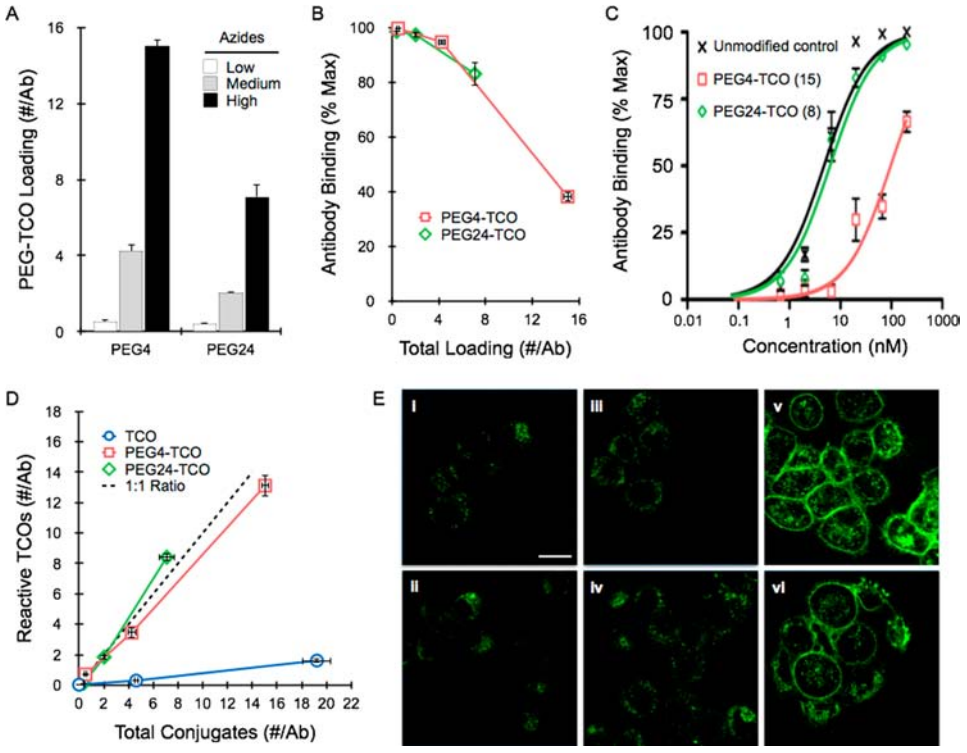

Figure 3. Introduction of TCO via PEG linkers using azide/DBCO reaction. (A) Attachment of heterobifunctional DBCO−PEG_n−TCO (n = 4 or 24) to azide-modified anti-EGFR antibodies. (B) Relative antibody binding at 10 μg/mL concentration showing that binding activity is retained up to ~8 linkers. (C) Kinetic binding curves after modification with PEG−TCOs. Binding affinity was unaffected for 8 PEG_{24}−TCOs (K_D = 6 nM), but it was significantly reduced for 15 PEG_4−TCOs (K_D =100 nM). (D) TCOs introduced via PEG linkers are fully reactive, as determined for live A431 cells labeled with modified antibodies and reacted with tetrazine−Oregon Green 488 by flow cytometry. (E) Confocal images of live A431 cancer cells labeled with (i, iii) no antibody or the anti-EGFR antibody modified with (ii) azide, (iv) TCO, (v) PEG_4−TCO, and (vi) PEG_{24}−TCO at the highest levels. Cells were then probed with (i, ii) DIBO−Alexa Fluor 488 or (iii−vi) tetrazine−Oregon Green 488 at 50 nM for 30 min. Scale bar: 20 μm. Error bars represent the standard error of at least three independent experiments.

extremely low concentration (50 nM) of tetrazine−Oregon Green 488 for 30 min at room temperature in the presence of 1 mg/mL BSA (Figure 3E). We similarly tested the anti-EGFR antibody modified with 15 azides followed by reaction with DIBO−Alexa Fluor 488. The TCO−PEG−antibodies yielded dramatically higher fluorescent signals than the TCO and azide cases, which were indistinguishable from autofluorescence. Thus, the PEG linkers effectively prevented TCO inactivation after antibody conjugation, presumably by increasing solubility and preventing interactions with the antibody while maintaining faster reaction kinetics than azide/DIBO. The PEG linkers should also be advantageous for *in vivo* applications by reducing antibody immunogenicity. A potential drawback is that higher rates of TCO inactivation by *trans*−*cis* isomerization have been reported in serum when using PEG linkers.[33] However, this study used a linker containing a phenyl group (benzyl ether) in between the TCO and a 12 subunit PEG. Therefore, it is possible that inactivation may not be as extensive for our carbonate linker that is more hydrophilic and 4 subunit PEG that is shorter.

A powerful application of tetrazine/TCO pretargeting is to amplify nanomaterial binding to cells and microvesicles.[17,18,20,22−27] Therefore, we labeled A431 cells with the TCO- and PEG−TCO-modified anti-EGFR antibodies and reacted with tetrazine-modified quantum dots (QD) at 10 nM concentration for 30 min. A QD immunoconjugate was also prepared and incubated under identical conditions. Fluorescence intensities measured by flow cytometry were similar for the QD immunoconjugate and TCO−antibody/tetrazine−QD cases (Figure 4A). Signals from both TCO−PEG−antibodies/tetrazine−QD cases were greater by as much as 6-fold. It should be noted that chemical amplification levels can increase further over immunoconjugates at higher nanoparticle concentrations.[17] These results were again entirely specific (Figure S5), and PEG length did not affect QD binding levels (Figure 4B). Improved detection capacity of the PEG_{24}−TCO was confirmed using confocal microscopy (Figure 4C).

Finally, we modified monoclonal antibodies specific for transferrin receptor (TfR) and EpCAM with TCO and PEG_{24}−TCO using the highest valency conditions. Functional and total modification levels were similar to the anti-EGFR antibody, and TCO reactivity was enhanced 3- to 4-fold using the PEG linker (Figure 5A). Binding of the TCO−PEG_{24}-modified anti-TfR antibody was slightly diminished, however (Figure S6). Similar 5-fold signal enhancements were observed by flow cytometry for both TCO−PEG_{24}−antibodies after reaction with tetrazine-modified QDs (Figure 5B). Improved detection capabilities were also demonstrated by confocal imaging using tetrazine-modified Oregon Green 488 (Figure S6) and QDs (Figure 5C). These results confirm that TCO masking after conjugation to monoclonal antibodies is not a rare phenomenon and that reactivity can reliably be improved by introducing via PEG linkers and our dual bioorthogonal coupling strategy.

DOI: 10.1021/bc500605g
Bioconjugate Chem. 2015, 26, 352−360

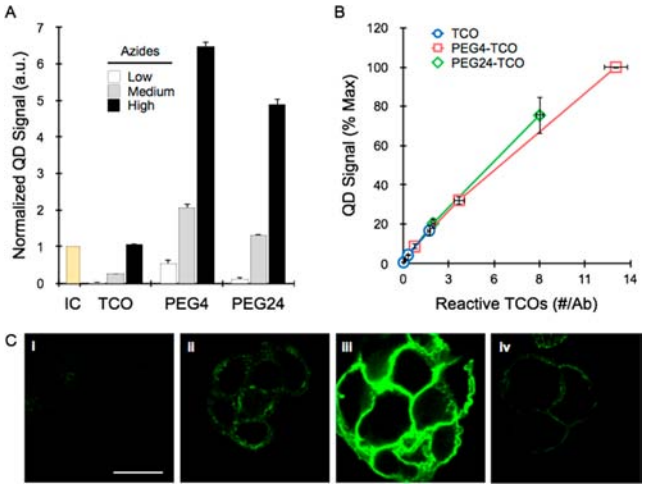

Figure 4. Amplification of QD binding. (A) QD signal determined by flow cytometry following cycloaddition reaction to modified anti-EGFR antibodies on A431 cancer cells. The TCO−PEG−antibodies displayed the highest binding levels, by as much as 6-fold for the PEG_4, over the TCO−antibody and the QD immunoconjugate. (B) QD binding levels correlated directly with the number of reactive TCOs, showing no influence of PEG length. (C) Confocal images of A431 cells labeled with (i, iv) no antibody or the anti-EGFR antibody conjugated with (ii) TCO or (iii) PEG_{24}−TCO. Cells were then probed with (i−iii) tetrazine−QD or (iv) QD immunoconjugate at 50 nM for 30 min. Scale bar: 20 μm. Error bars represent the standard error of at least three independent experiments.

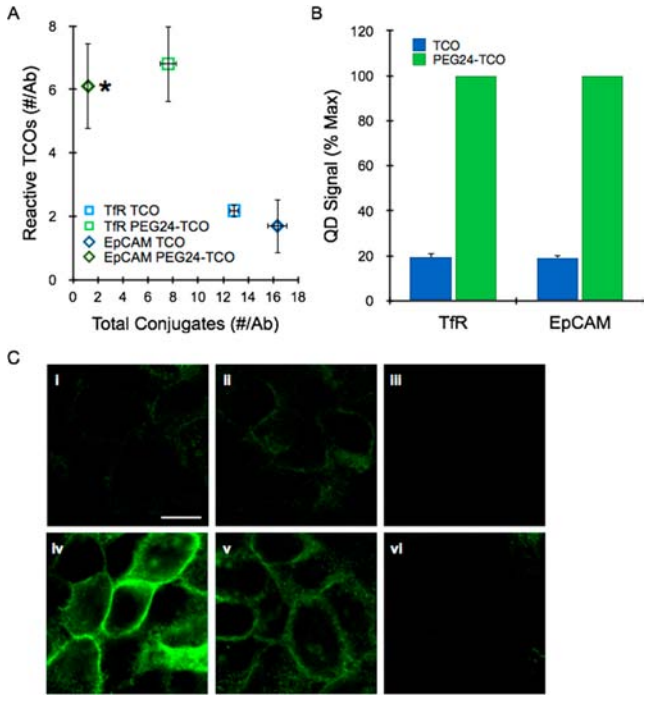

Figure 5. Translation of dual orthogonal coupling to different antibodies. (A) Anti-TfR and EpCAM antibodies had low TCO reactivity (12−15%) after direct amine-conjugation, but the PEG_{24}−TCO increased reactive TCO density 3- to 4-fold. *MALDI-TOF analysis of the TCO−PEG_{24}-modified anti-EpCAM antibody was limited by difficulties with desorption. (B) Flow cytometry results for TCO- and TCO−PEG_{24}-modified anti-EpCAM and TfR antibodies on A431 cells after reaction with 10 nM tetrazine−QDs for 30 min, showing 5-fold signal enhancements for the PEG_{24}−TCO. (C) Confocal images of A431 cells labeled with (i, iv) anti-EpCAM, (ii, v) anti-TfR, or (iii, vi) nonbinding control antibodies. The antibodies were modified with (i−iii) TCO or (iv−vi) PEG_{24}−TCO at the highest densities and reacted with tetrazine−QD at 10 nM for 30 min. Scale bar: 20 μm. Error bars represent the standard error of at least three independent experiments.

CONCLUSIONS

In this work, we have discovered that the majority of TCOs conjugated to antibodies using standard amine-coupling procedures are nonreactive. To address this issue, we introduced TCO via hydrophilic PEG linkers, which fully preserved reactivity and improved detection signals for tetrazine-modified fluorophores and quantum dots. Taken together with other evidence presented, we believe that nonfunctional TCOs are buried within the antibody. This likely occurs during conjugation procedures, as TCO reactivity is later maintained in the presence of cells and high concentrations of BSA protein. We believe this work establishes a new method to prepare TCO-modified antibodies that will significantly advance bioorthogonal pretargeting studies such as *in vivo* imaging and chemical amplification of nanoparticle binding. Additionally, this technique could be useful for signal amplification of activatable fluorochromes.[42−45] Although we utilized azide/DBCO cycloaddition reaction to couple PEG−TCO to antibodies, we expect that direct amine-reaction or alternative chemistries should provide similar results. Future work could explore whether similar masking effects occur for different hydrophobic reactants such as DBCO, norbornene, and methyl-cyclopropene, alternative linkers directly distal to the TCO such as those containing bulky phenyl groups,[16] or new bicyclic TCO derivatives that have faster reaction rates, greater stability, and, for the dioxolane-fused TCO, potentially greater hydrophilicity.[46,47] Expanding these investigations to different types of proteins or biological molecules, including site-specific methods that involve genetic encoding,[48−50] would also be of interest.

EXPERIMENTAL PROCEDURES

Materials. All chemicals were purchased from Sigma-Aldrich unless noted and were used as received. The DBCO−amine was purchased from Click Chemistry Tools (Scottsdale, AZ). Heterobifunctional carboxy−$(PEG)_n$−amine with n = 4 or 24 subunits and amine-reactive succinimidyl ester (NHS)-azide were purchased from Thermo Fisher Scientific (Rockford, IL). Primary amine-terminated quantum dots (Qdot 605 ITK Amino), Alexa Fluor 488 DIBO Alkyne, and amine-reactive NHS−Oregon Green 488 were purchased from Life Technologies (Grand Island, NY). Monoclonal mouse antibodies specific for human EpCAM (IgG_{2b}, clone 158206) and transferrin receptor (TfR, IgG_1, clone 29806) were purchased from R&D Systems (Minneapolis, MN). A non-binding isotope control antibody (mouse IgG_1, clone MOPC-21) was purchased from BioLegend (San Diego, CA). All solvents were of reagent grade or higher and were used without further purification. HR MS (ESI LC-TOF) and MALDI-TOF (matrix-assisted laser desorption ionization-time-of-flight) mass spectrometry were performed for characterization of hetero-bifunctional PEG linkers and antibodies, respectively. HR MS was performed using a Waters LCT Premier system. For all HR MS measurements, product was dissolved in methanol.

DOI: 10.1021/bc500605g
Bioconjugate Chem. 2015, 26, 352−360

MALDI-TOF was performed using a AB SCIEX TOF/TOF 5800 system with a MALDI matrix composed of 1 mg of sinapinic acid dissolved in 100 μL of 70:30 acetonitrile/water with 0.1% trifluororacetic acid. Absorption measurements were recorded on a Thermo Scientific NanoDrop 2000 spectrophotometer. All kinetic binding analyses were performed using GraphPad Prism. Synthesis of tetrazine−amine, NHS−tetrazine, tetrazine−Oregon Green 488, and NHS−TCO were as previously reported.[29−31]

Synthesis of DBCO−PEG−TCO Linkers. Heterobifunctional DBCO−PEG_n−TCO linkers were synthesized from a carboxylic acid−PEG_n−amine: 100 mg of carboxylic acid−PEG_n−amine was reacted with 2 equiv of TCO−NHS in 2 mL of DCM containing 1.5 equiv of triethylamine for 16 h on ice. This reaction mixture was purified using silica column chromatography with a DCM/methanol gradient. The product reacted with *N,N′*-disuccinimidyl carbonate in triethylamine overnight to form NHS−PEG_n−TCO. After evaporation, DBCO was coupled by reacting NHS−PEG_n−TCO with 1.5 equiv of amine-DBCO in 2 mL DCM containing 1.5 equiv of triethylamine overnight. The final DBCO−PEG_n−TCO was purified using silica column chromatography with a DCM/methanol gradient for the PEG_4 linker or using Sephedex G-10 desalting media for the PEG_{24} linker. DBCO−PEG_4−TCO was verified by proton NMR. Both linkers where characterized by HR MS with ESI-LC-TOF. Purified product was dissolved in methanol and loaded into Waters LCT Premier system and analyzed by Waters MassLynx (Version 4.0). DBCO−PEG_4−TCO: ^{1}H NMR (400 MHz, $CDCl_3$) δ 7.71−7.73 (d, 1H), 7.44−7.45 (m, 6H), 7.33 (d, 1H), 6.94 (s, 1H), 5.55−5.72 (m, 2H), 5.30 (d, 1H), 5.10−5.20 (m, 1H), 4.38 (s, 1H), 3.56−3.73 (m, 14H), 3.33−3.56 (m, 4H), 2.73−2.76 (m, 8H), 2.40−2.41 (m, 3H), 1.95−2.04 (m, 3H), 1.77 (m, 2H), 1.59 (m, 1H). HRMS (TOF MS ES+) calcd for $C_{38}H_{49}N_3O_8Na$, 698.3520; found, 698.3418. DBCO−PEG_{24}−TCO: TOF MS [M + Na] calcd for $C_{78}H_{129}N_3O_{28}Na$, 1578.87; found, 1579.03.

Anti-EGFR Antibody Production from Hybridoma. Monoclonal mouse antibody specific for human EGFR (IgG_{2a}, clone Mab 108) was produced from hybridoma HB-9764 obtained from ATCC (Manassas, VA). Hybridoma cells were grown in RPMI media containing 10% fetal bovine serum, 5% penicillin/streptomycin, 5% L-glutamine, and 1% sodium pyruvate and subcultured by dilution of the nonadherent cells. For antibody production, 500 mL hybridoma cell cultures were grown for 7 days from an initial seeding density of 5×10^5 cells/mL. The media was collected, centrifuged at 3000*g* for 10 min to remove cell debris, concentrated, buffer-exchanged into PBS using a Labscale tangential flow filtration system fitted with a Pellicon XL cassette (both from Millipore, Billerica, MA), and purified using a HiTrap Protein G column (GE Healthcare, Piscataway, NJ).

Antibody Modifications. Anti-EGFR, anti-EpCAM, anti-TfR, and nonbinding control antibodies were buffer-exchanged into PBS using Zeba spin desalting columns (Thermo Scientific) prior to modification. Direct TCO conjugates was prepared by reacting 200 μg of antibody with 10, 100, or 1000 equiv of NHS−TCO in 0.2 mL PBS containing 10% DMF and 0.1 M $NaHCO_3$ (pH 8.5) for 3 h at room temperature. Azide and Oregon Green 488A conjugates were prepared in a similar manner using 10, 30, or 100 equiv of NHS-azide or 10 equiv of NHS−Oregon Green 488, with DMF omitted from the solvent. To study the effect of DMF on total TCO conjugation, direct TCO conjugates were also prepared in PBS containing <1% or <5% DMF for reaction with 100 or 1000 equiv of NHS−TCO, respectively. TCO, azide, and Oregon Green 488-modified antibodies were purified using Zeba spin desalting columns. PEG−TCO conjugates were prepared by reacting the different azide-modified antibodies with DBCO−PEG−TCO molecules containing 4 or 24 subunits. Reactions were carried out using 10-fold excess relative to the number of azide moieties for 4 h at room temperature. TCO−PEG−antibodies were purified into PBS using Amicon Ultra-4 centrifugal filtration systems (Millipore). Antibody concentration was determined by absorption measurement. Oregon Green 488 density was also measured by absorption to be 2 dyes/antibody.

Cell Culture. Human epidermoid cancer cell line A431 and hybridoma HB-9764 producing mouse anti-human EGFR antibody clone MAb108 were obtained from ATCC (Manassas, VA). A431 cells were selected for antibody labeling studies due to high-level expression of EGFR and EpCAM biomarkers as well as moderate expression of TfR. Cells were cultured in flasks at 37 °C with 5% CO_2. A431 cells were grown in DMEM media containing 10% fetal bovine serum, 5% penicillin/streptomycin, and 5% L-glutamine and subcultured after reaching confluence by treatment with trypsin−EDTA (Corning, NY).

MALDI-TOF Analysis of Modified Antibodies. Total TCO and azide densities were determined based on changes in mass using MALDI-TOF mass spectrometry. The matrix was prepared using 1 mg of sinapinic acid dissolved in 100 μL of 70:30 acetonitrile/water with 0.1% trifluororacetic acid. Unmodified control and TCO-, TCO-PEG-, and azide-modified antibodies were buffer-exchanged into water and concentrated to greater than 1 mg/mL using Amicon Ultra-4 centrifugal filters (Millipore). Concentrated antibody solutions were combined with sinapinic acid matrix in a 2:1 ratio, and 1 μL of the solution was dried on a sample plate. The sample was loaded onto a AB SCIEX TOF/TOF 5800 MALDI-TOF spectrometer to obtain an average molecular weight for each antibody. Data was acquired using AB SCIEX Analyst software and exported to MatLab (MathWorks). The number of modifications per antibody was then calculated based on the difference in molecular weight compared to the unmodified antibody and assuming a specific net mass added depending on the modification. Direct azide and TCO modifications had expected masses of 83.0 and 152.2 g/mol, respectively. TCO−PEG linker modifications with 4 and 24 PEG subunits had expected masses of 758.2 and 1639.9 g/mol, respectively.

Measurement of TCO and Azide Reactivities on Antibodies. Functional TCO loadings were measured for direct TCO-modified antibodies using tetrazine−Oregon Green 488. Azide-modified antibodies were similarly assessed using DIBO−Alexa Fluor 488. Reactions were performed using 100 μg of antibody and 50 μM reactive dye in PBS containing 5% DMF at room temperature for 4 h. To study the mechanism of TCO inactivation, reaction of direct TCO-modified antibodies with tetrazine−Oregon Green 488 were also performed in PBS containing 10% DMF or PBS containing 5% DMF and 5% DMSO. All samples were purified into PBS using Zeba spin desalting columns, and the number of fluorophores per antibody was determined by absorption measurements.

Analysis of Antibody Binding. A431 cells (500 000 cells/sample) were fixed using 4% formaldehyde (Sigma) in PBS and washed using PBS. Binding experiments involved an indirect assay since secondary antibodies may no longer recognize the

DOI: 10.1021/bc500605g
Bioconjugate Chem. 2015, 26, 352−360

modified antibodies, particularly for the TCO−PEG cases. This involved labeling cells with unmodified and azide-, TCO-, and TCO−PEG-modified antibodies at concentrations ranging from 0.6 to 200 nM in 100 μL of PBS containing 1 mg/mL bovine serum albumin (PBS+) for 30 min at room temperature. After washing 3 times with ice-cold PBS+ by centrifugation, samples were incubated with Oregon Green 488-modified antibody at 10 μg/mL in 100 μL of PBS+ for 30 min on ice and again washed 3 times. Finally, fluorescence was assessed using an LSRII flow cytometer (BD Biosciences, San Jose, CA) and analyzed using FlowJo software (Tree Star, Ashland, OR). The ability of the first antibody to block the Oregon Green 488-labeled antibody is representative of binding activity. Fully blocked conditions were indicated by the signal obtained for the unmodified antibody, and the fully unblocked condition was represented by cells treated only with the Oregon Green 488-labeled antibody. Specifically, the mean fluorescence intensity was subtracted from values obtained for cells incubated only with Oregon Green 488−antibody, and all samples were then normalized to the unmodified control (100%).

Preparation of Quantum Dots. Amine-terminated quantum dots (QDs) were modified with NHS−tetrazine as described previously.[18] QDs were first buffer-exchanged into PBS using Amicon Ultra-4 centrifugal devices. The reaction was performed using 0.8 nmoles of QD and 500 mol equiv of NHS−tetrazine in PBS containing 5% DMF and 0.01 M $NaHCO_3$ for 3 h at room temperature. Tetrazine−QDs were purified into PBS using centrifugal filters. To prepare QD immunoconjugates, 200 μg of antibody was modified with 10 mol equiv of TCO−NHS, buffer-exchanged using a Zeba column, and reacted with 0.15 nmoles of tetrazine−QD in 1 mL of PBS+ for 3 h at room temperature. QD immunoconjugates were purified with Sephacryl S-400 (GE Healthcare) in PBS using a AKTA Pure FPLC (GE Healthcare). Final concentrations were determined by absorption measurements using the QD stock solution for calibration.

Quantification of Cell Labeling Using Flow Cytometry. A431 cells (500 000 cells/sample) were labeled with TCO- or TCO−PEG-modified antibodies at saturating or near-saturating concentrations (10−30 μg/mL) in 100 μL of PBS+ for 30 min at room temperature. Cells were then washed 3 times by centrifugation with PBS+, reacted with 50 μM tetrazine−Oregon Green 488 or 10 nM tetrazine−quantum dots for 30 min at room temperature, and washed 3 times by centrifugation with ice-cold PBS+. Fluorescence intensities were assessed by flow cytometry and analyzed using FlowJo software. Cells treated with no primary antibody, TCO-modified nonbinding control, or TCO−PEG24-modified nonbinding control antibody were used for controls. The number of reactive TCOs for the TCO−PEG-modified antibodies was determined based on fluorescence intensity of the Oregon Green 488, relative to the signal from the TCO-modified antibodies that were directly assessed for TCO reactivity previously. Adjustments were made for antibody binding level to obtain true representations of the number of reactive TCOs per antibody.

Confocal Imaging. A431 cells were grown on Lab-Tek glass chamber slides (Rochester, NY). Prior to experiments, samples were washed with PBS+ and labeled with TCO-, TCO−PEG, or azide-modified antibodies under saturating or near-saturating concentrations (10−30 μg/mL) for 30 min at room temperature. After washing with PBS+, cells were labeled with tetrazine−Oregon Green 488 or DIBO−Alexa Fluor 488 at 50 nM or tetrazine−quantum dots at 10 nM for 30 min at room temperature. Cells were then washed and imaged using an inverted laser scanning confocal microscope (FV1000, Olympus) with a 60× water immersion lens, and data was acquired with Fluoview software (Olympus).

■ ASSOCIATED CONTENT

Supporting Information

Characterization of the heterobifunctional DBCO−PEG−TCO linker, MALDI-TOF results for all antibodies, investigation of solvent concentration during antibody conjugation and TCO reaction, binding analysis of modified antibodies, and background signals from tetrazine-modified probes. This material is available free of charge via the Internet at http://pubs.acs.org.

■ AUTHOR INFORMATION

Corresponding Author

*Phone: 949-824-1243 E-mail: jered.haun@uci.edu.

Notes

The authors declare no competing financial interest.

■ ACKNOWLEDGMENTS

We thank Dr. Sumi Lee for synthetic assistance and Dr. Hongtao Chen for help with confocal imaging studies that were performed at the Laboratory for Fluorescence Dynamics (LFD) at the University of California Irvine. The LFD is supported jointly by the National Institute of General Medical Sciences of the National Institutes of Health under award no. 8P41GM103540 grant and the University of California Irvine. This work was also supported in part by the National Cancer Institute of the National Institutes of Health under award no. P30CA062203 and the Interdisciplinary Innovation Initiative in the Henry Samueli School of Engineering at the University of California Irvine.

■ REFERENCES

(1) Devaraj, N. K., and Weissleder, R. (2011) Biomedical applications of tetrazine cycloadditions. *Acc. Chem. Res. 44*, 816−827.

(2) Sletten, E. M., and Bertozzi, C. R. (2011) From mechanism to mouse: a tale of two bioorthogonal reactions. *Acc. Chem. Res. 44*, 666−676.

(3) Seckute, J., and Devaraj, N. K. (2013) Expanding room for tetrazine ligations in the in vivo chemistry toolbox. *Curr. Opin. Chem. Biol. 17*, 761−767.

(4) Selvaraj, R., and Fox, J. M. (2013) *trans*-Cyclooctene—a stable, voracious dienophile for bioorthogonal labeling. *Curr. Opin. Chem. Biol. 17*, 753−760.

(5) Rahim, M. K., Kota, R., Lee, S., and Haun, J. B. (2013) Bioorthogonal chemistries for nanomaterial conjugation and targeting. *Nanotechnol. Rev. 2*, 215−227.

(6) Rossin, R., and Robillard, M. S. (2014) Pretargeted imaging using bioorthogonal chemistry in mice. *Curr. Opin. Chem. Biol. 21C*, 161−169.

(7) Carroll, L., Evans, H. L., Aboagye, E. O., and Spivey, A. C. (2013) Bioorthogonal chemistry for pre-targeted molecular imaging—progress and prospects. *Org. Biomol. Chem. 11*, 5772−5781.

(8) Rossin, R., Verkerk, P. R., van den Bosch, S. M., Vulders, R. C., Verel, I., Lub, J., and Robillard, M. S. (2010) *In vivo* chemistry for pretargeted tumor imaging in live mice. *Angew. Chem., Int. Ed. 49*, 3375−3378.

(9) Devaraj, N. K., Thurber, G. M., Keliher, E. J., Marinelli, B., and Weissleder, R. (2012) Reactive polymer enables efficient *in vivo* bioorthogonal chemistry. *Proc. Natl. Acad. Sci. U.S.A. 109*, 4762−4767.

DOI: 10.1021/bc500605g
Bioconjugate Chem. 2015, 26, 352−360

(10) Zeglis, B. M., Sevak, K. K., Reiner, T., Mohindra, P., Carlin, S. D., Zanzonico, P., Weissleder, R., and Lewis, J. S. (2013) A pretargeted PET imaging strategy based on bioorthogonal Diels−Alder click chemistry. *J. Nucl. Med. 54*, 1389−1396.
(11) Emmetiere, F., Irwin, C., Viola-Villegas, N. T., Longo, V., Cheal, S. M., Zanzonico, P., Pillarsetty, N., Weber, W. A., Lewis, J. S., and Reiner, T. (2013) ^{18}F-labeled-bioorthogonal liposomes for *in vivo* targeting. *Bioconjugate Chem. 24*, 1784−1789.
(12) Rossin, R., Lappchen, T., van den Bosch, S. M., Laforest, R., and Robillard, M. S. (2013) Diels−Alder reaction for tumor pretargeting: *in vivo* chemistry can boost tumor radiation dose compared with directly labeled antibody. *J. Nucl. Med. 54*, 1989−1995.
(13) Lee, S. B., Kim, H. L., Jeong, H. J., Lim, S. T., Sohn, M. H., and Kim, D. W. (2013) Mesoporous silica nanoparticle pretargeting for PET imaging based on a rapid bioorthogonal reaction in a living body. *Angew. Chem., Int. Ed. 52*, 10549−10552.
(14) Wyffels, L., Thomae, D., Waldron, A. M., Fissers, J., Dedeurwaerdere, S., Van der Veken, P., Joossens, J., Stroobants, S., Augustyns, K., and Staelens, S. (2014) *In vivo* evaluation of ^{18}F-labeled TCO for pre-targeted PET imaging in the brain. *Nucl. Med. Biol. 41*, 513−523.
(15) Zlitni, A., Janzen, N., Foster, F. S., and Valliant, J. F. (2014) Catching bubbles: targeting ultrasound microbubbles using bioorthogonal inverse-electron-demand Diels−Alder reactions. *Angew. Chem., Int. Ed. 53*, 6459−6463.
(16) Rossin, R., van Duijnhoven, S. M., Lappchen, T., van den Bosch, S. M., and Robillard, M. S. (2014) *Trans*-cyclooctene tag with improved properties for tumor pretargeting with the Diels−Alder reaction. *Mol. Pharmaceutics 11*, 3090−3096.
(17) Haun, J. B., Devaraj, N. K., Hilderbrand, S. A., Lee, H., and Weissleder, R. (2010) Bioorthogonal chemistry amplifies nanoparticle binding and enhances the sensitivity of cell detection. *Nat. Nanotechnol. 5*, 660−665.
(18) Haun, J. B., Devaraj, N. K., Marinelli, B. S., Lee, H., and Weissleder, R. (2011) Probing intracellular biomarkers and mediators of cell activation using nanosensors and bioorthogonal chemistry. *ACS Nano 5*, 3204−3213.
(19) Haun, J. B., Castro, C. M., Wang, R., Peterson, V. M., Marinelli, B. S., Lee, H., and Weissleder, R. (2011) Micro-NMR for rapid molecular analysis of human tumor samples. *Sci. Transl. Med. 3*, 71ra16.
(20) Liong, M., Fernandez-Suarez, M., Issadore, D., Min, C., Tassa, C., Reiner, T., Fortune, S. M., Toner, M., Lee, H., and Weissleder, R. (2011) Specific pathogen detection using bioorthogonal chemistry and diagnostic magnetic resonance. *Bioconjugate Chem. 22*, 2390−2394.
(21) Chung, H. J., Reiner, T., Budin, G., Min, C., Liong, M., Issadore, D., Lee, H., and Weissleder, R. (2011) Ubiquitous detection of Gram-positive bacteria with bioorthogonal magnetofluorescent nanoparticles. *ACS Nano 5*, 8834−8841.
(22) Issadore, D., Chung, J., Shao, H., Liong, M., Ghazani, A. A., Castro, C. M., Weissleder, R., and Lee, H. (2012) Ultrasensitive clinical enumeration of rare cells *ex vivo* using a micro-Hall detector. *Sci. Transl. Med. 4*, 141ra92.
(23) Ghazani, A. A., Castro, C. M., Gorbatov, R., Lee, H., and Weissleder, R. (2012) Sensitive and direct detection of circulating tumor cells by multimarker micro-nuclear magnetic resonance. *Neoplasia 14*, 388−395.
(24) Shao, H., Chung, J., Balaj, L., Charest, A., Bigner, D. D., Carter, B. S., Hochberg, F. H., Breakefield, X. O., Weissleder, R., and Lee, H. (2012) Protein typing of circulating microvesicles allows real-time monitoring of glioblastoma therapy. *Nat. Med. 18*, 1835−1840.
(25) Rho, J., Chung, J., Im, H., Liong, M., Shao, H., Castro, C. M., Weissleder, R., and Lee, H. (2013) Magnetic nanosensor for detection and profiling of erythrocyte-derived microvesicles. *ACS Nano 7*, 11227−11233.
(26) Ghazani, A. A., McDermott, S., Pectasides, M., Sebas, M., Mino-Kenudson, M., Lee, H., Weissleder, R., and Castro, C. M. (2013) Comparison of select cancer biomarkers in human circulating and bulk tumor cells using magnetic nanoparticles and a miniaturized micro-NMR system. *Nanomedicine 9*, 1009−1017.
(27) Ghazani, A. A., Pectasides, M., Sharma, A., Castro, C. M., Mino-Kenudson, M., Lee, H., Shepard, J. A., and Weissleder, R. (2014) Molecular characterization of scant lung tumor cells using iron-oxide nanoparticles and micro-nuclear magnetic resonance. *Nanomedicine 10*, 661−668.
(28) Blackman, M. L., Royzen, M., and Fox, J. M. (2008) Tetrazine ligation: fast bioconjugation based on inverse-electron-demand Diels−Alder reactivity. *J. Am. Chem. Soc. 130*, 13518−13519.
(29) Devaraj, N. K., Upadhyay, R., Haun, J. B., Hilderbrand, S. A., and Weissleder, R. (2009) Fast and sensitive pretargeted labeling of cancer cells through a tetrazine/*trans*-cyclooctene cycloaddition. *Angew. Chem., Int. Ed. 48*, 7013−7016.
(30) Devaraj, N. K., Weissleder, R., and Hilderbrand, S. A. (2008) Tetrazine-based cycloadditions: application to pretargeted live cell imaging. *Bioconjugate Chem. 19*, 2297−2299.
(31) Yang, J., Seckute, J., Cole, C. M., and Devaraj, N. K. (2012) Live-cell imaging of cyclopropene tags with fluorogenic tetrazine cycloadditions. *Angew. Chem., Int. Ed. 51*, 7476−7479.
(32) Patterson, D. M., Nazarova, L. A., Xie, B., Kamber, D. N., and Prescher, J. A. (2012) Functionalized cyclopropenes as bioorthogonal chemical reporters. *J. Am. Chem. Soc. 134*, 18638−18643.
(33) Rossin, R., van den Bosch, S. M., Ten Hoeve, W., Carvelli, M., Versteegen, R. M., Lub, J., and Robillard, M. S. (2013) Highly reactive *trans*-cyclooctene tags with improved stability for Diels−Alder chemistry in living systems. *Bioconjugate Chem. 24*, 1210−1217.
(34) Yang, J., Liang, Y., Seckute, J., Houk, K. N., and Devaraj, N. K. (2014) Synthesis and reactivity comparisons of 1-methyl-3-substituted cyclopropene mini-tags for tetrazine bioorthogonal reactions. *Chemistry 20*, 3365−3375.
(35) Chapman, A. P. (2002) PEGylated antibodies and antibody fragments for improved therapy: a review. *Adv. Drug Delivery Rev. 54*, 531−545.
(36) Villaraza, A. J., Milenic, D. E., and Brechbiel, M. W. (2010) Improved speciation characteristics of PEGylated indocyanine green-labeled panitumumab: revisiting the solution and spectroscopic properties of a near-infrared emitting anti-HER1 antibody for optical imaging of cancer. *Bioconjugate Chem. 21*, 2305−2312.
(37) Sano, K., Nakajima, T., Miyazaki, K., Ohuchi, Y., Ikegami, T., Choyke, P. L., and Kobayashi, H. (2013) Short PEG-linkers improve the performance of targeted, activatable monoclonal antibody-indocyanine green optical imaging probes. *Bioconjugate Chem. 24*, 811−816.
(38) Suzuki, T., Kanbara, N., Tomono, T., Hayashi, N., and Shinohara, I. (1984) Physicochemical and biological properties of poly(ethylene glycol)-coupled immunoglobulin G. *Biochim. Biophys. Acta 788*, 248−255.
(39) Kitamura, K., Takahashi, T., Yamaguchi, T., Noguchi, A., Noguchi, A., Takashina, K., Tsurumi, H., Inagake, M., Toyokuni, T., and Hakomori, S. (1991) Chemical engineering of the monoclonal antibody A7 by polyethylene glycol for targeting cancer chemotherapy. *Cancer. Res. 51*, 4310−4315.
(40) Hapuarachchige, S., Zhu, W., Kato, Y., and Artemov, D. (2014) Bioorthogonal, two-component delivery systems based on antibody and drug-loaded nanocarriers for enhanced internalization of nanotherapeutics. *Biomaterials 35*, 2346−2354.
(41) Karver, M. R., Weissleder, R., and Hilderbrand, S. A. (2012) Bioorthogonal reaction pairs enable simultaneous, selective, multi-target imaging. *Angew. Chem., Int. Ed. 51*, 920−922.
(42) Devaraj, N. K., Hilderbrand, S., Upadhyay, R., Mazitschek, R., and Weissleder, R. (2010) Bioorthogonal turn-on probes for imaging small molecules inside living cells. *Angew. Chem., Int. Ed. 49*, 2869−2872.
(43) Carlson, J. C., Meimetis, L. G., Hilderbrand, S. A., and Weissleder, R. (2013) BODIPY−tetrazine derivatives as superbright bioorthogonal turn-on probes. *Angew. Chem., Int. Ed. 52*, 6917−6920.

DOI: 10.1021/bc500605g
Bioconjugate Chem. 2015, 26, 352−360

(44) Meimetis, L. G., Carlson, J. C., Giedt, R. J., Kohler, R. H., and Weissleder, R. (2014) Ultrafluorogenic coumarin-tetrazine probes for real-time biological imaging. *Angew. Chem., Int. Ed. 53*, 7531−7534.
(45) Wu, H., Cisneros, B. T., Cole, C. M., and Devaraj, N. K. (2014) Bioorthogonal tetrazine-mediated transfer reactions facilitate reaction turnover in nucleic acid-templated detection of microRNA. *J. Am. Chem. Soc. 136*, 17942−17945.
(46) Taylor, M. T., Blackman, M. L., Dmitrenko, O., and Fox, J. M. (2011) Design and synthesis of highly reactive dienophiles for the tetrazine−*trans*-cyclooctene ligation. *J. Am. Chem. Soc. 133*, 9646−9649.
(47) Darko, A., Wallace, S., Dmitrenko, O., Machinova, M. M., Mehl, R. A., Chin, J. W., and Fox, J. M. (2014) Conformationally strained *trans*-cyclooctene with improved stability and excellent reactivity in tetrazine ligation. *Chem. Sci. 5*, 3770−3776.
(48) Lang, K., Davis, L., Torres-Kolbus, J., Chou, C., Deiters, A., and Chin, J. W. (2012) Genetically encoded norbornene directs site-specific cellular protein labelling via a rapid bioorthogonal reaction. *Nat. Chem. 4*, 298−304.
(49) Lang, K., Davis, L., Wallace, S., Mahesh, M., Cox, D. J., Blackman, M. L., Fox, J. M., and Chin, J. W. (2012) Genetic Encoding of bicyclononynes and *trans*-cyclooctenes for site-specific protein labeling *in vitro* and in live mammalian cells via rapid fluorogenic Diels−Alder reactions. *J. Am. Chem. Soc. 134*, 10317−10320.
(50) Nikic, I., Plass, T., Schraidt, O., Szymanski, J., Briggs, J. A., Schultz, C., and Lemke, E. A. (2014) Minimal tags for rapid dual-color live-cell labeling and super-resolution microscopy. *Angew. Chem., Int. Ed. 53*, 2245−2249.

DOI: 10.1021/bc500605g
Bioconjugate Chem. 2015, 26, 352−360